Heliyon 10 (2024) e32743

Contents lists available at ScienceDirect

Heliyon

journal homepage: www.cell.com/heliyon

Research article

# Interaction between RNF4 and SART3 is associated with the risk of schizophrenia

Ying Cheng [a,b,1], Xi Chen [a,b,1], Xiao Qing Zhang [a,b,1], Pei Jun Ju [a], Wei Di Wang [a,c], Yu Fang [a,b], Guan Ning Lin [a,c,**], Dong Hong Cui [a,b,d,*]

[a] Shanghai Mental Health Center, Shanghai Jiao Tong University School of Medicine, Shanghai, China
[b] Shanghai Key Laboratory of Psychotic Disorders, Shanghai, China
[c] Division of Imaging, Computational and Systems Biomedicine, School of Biomedical Engineering & Med-X Research Institute, Shanghai Jiao Tong University, Shanghai, China
[d] Brain Science and Technology Research Center, Shanghai Jiao Tong University, Shanghai, China

ARTICLE INFO

*Keywords:*
Schizophrenia
Ring finger protein 4
Squamous cell carcinoma antigen recognized by T cells 3
Single-nucleotide polymorphism

ABSTRACT

The pathogenesis of schizophrenia (SCZ) is heavily influenced by genetic factors. Ring finger protein 4 (*RNF4*) and squamous cell carcinoma antigen recognized by T cells 3 (*SART3*) are thought to be involved in nervous system growth and development via oxidative stress pathways. Moreover, they have previously been linked to SCZ. Yet the role of *RNF4* and *SART3* in SCZ remains unclear. Here, we investigated how these two genes are involved in SCZ by studying their variants observed in patients. We first observed significantly elevated mRNA levels of *RNF4* and *SART3* in the peripheral blood in both first-episode (n = 30) and chronic (n = 30) SCZ patients compared to controls (n = 60). Next, we targeted-sequenced three single nucleotide polymorphisms (SNPs) in *SART3* and six SNPs in *RNF4* for association with SCZ using the genomic DNA extracted from peripheral blood leukocytes from SCZ participants (n = 392) and controls (n = 572). We observed a combination of SNPs that included rs1203860, rs2282765 (both in *RNF4*), and rs2287550 (in *SART3*) was associated with increased risk of SCZ, suggesting common pathogenic mechanisms between these two genes. We then conducted experiments in HEK293T cells to better understand the interaction between RNF4 and SART3. We observed that SART3 lowered the expression of RNF4 through ubiquitination and downregulated the expression of nuclear factor E2-related factor 2 (NRF2), a downstream factor of RNF4, implicating the existence of a possible shared regulatory mechanism for RNF4 and SART3. In conclusion, our study provides evidence that the interaction between *RNF4* and *SART3* contributes to the risk of SCZ. The findings shed light on the underlying molecular mechanisms of SCZ and may lead to the development of new therapies and interventions for this disorder.

## 1. Introduction

Schizophrenia (SCZ) is a complex disorder influenced by both genetic and environmental factors [1,2]. Numerous single nucleotide

* Corresponding author. Shanghai Mental Health Center Shanghai Jiao Tong University School of Medicine Shanghai, TEL, China.
** Corresponding author. Shanghai Mental Health Center, Shanghai Jiao Tong University School of Medicine, Shanghai, TEL, China.
*E-mail addresses:* nickgnlin@sjtu.edu.cn (G.N. Lin), manyucc@126.com (D.H. Cui).
[1] Equal contributions.

https://doi.org/10.1016/j.heliyon.2024.e32743
Received 8 September 2023; Received in revised form 3 June 2024; Accepted 7 June 2024
Available online 8 June 2024

polymorphisms (SNPs) have been identified in antecedent investigations [3], especially in recent years. Noteworthy among these are novel SNPs, such as those manifesting in P2X purinoceptor 4 (*P2XR4*) [4], GABAA receptor β2 subunit gene (*GABRB2*) [5], Kinesin Family Member 26B (*KIF26B*) [6], Peroxisome proliferator-activated receptor-γ (*PPARG*) [7], and Grainyhead-like transcription factors 3 (*GRHL3*) [8]. These SNPs have been posited as putative risk factors for SCZ, given their involvement in pathways pertinent to brain development and neuronal functionality. Nevertheless, a comprehensive understanding of the genetic mechanisms of this disorder remains elusive.

Recent research has implicated the Ring finger protein 4 (*RNF4*) and Squamous cell carcinoma antigen recognized by T cells 3 (*SART3*) genes in the pathogenesis of SCZ [9,10], given their roles in central nervous system (CNS) development and pathophysiology. *RNF4* is located on chromosome 4p16.3 [11], encoding a small ubiquitin-like modifier (SUMO)-targeted ubiquitin E3 ligase. It is predominantly expressed in the developing nervous system as a key transcriptional regulator involved in early brain development [12]. In addition, RNF4 mediates the degradation of misfolded proteins in a SUMOylation-dependent manner, thus protecting neurons from injury [13]. The degradation of its downstream target, NF-E2-related factor 2 (NRF2), is also mediated by RNF4. They play pivotal roles in antioxidant defense pathways [14]. *SART3*, located on chromosome 12q23.3 [15], is a developmental gene involved in the growth, survival, and differentiation of embryonic stem cells [16,17], with important roles in the CNS [18]. Previous studies have demonstrated that mutations or deletions of *RNF4* and *SART3* genes can result in embryonic lethality or abnormalities of CNS development in animal models [18–21].

Clinical studies have revealed the presence of de novo mutations in *RNF4* and *SART3* genes in patients with SCZ and other neuropsychiatric disorders [10,22]. Moreover, our previous study demonstrated differential expression of the *RNF4* and *SART3* genes in the blood of patients with SCZ compared to controls [9], which suggested their potential involvement in the pathogenesis of SCZ.

Our present study seeks to delve deeper into the potential influence of *RNF4* and *SART3* gene polymorphisms on the risk of SCZ. We analyzed the association between *RNF4* and *SART3* SNPs and susceptibility to SCZ. Furthermore, we explored the biological regulation of RNF4 and SART3 within signaling pathways using HEK293T cells. Our study elucidates a two-gene collaborative model that amplifies the susceptibility to SCZ, presenting novel avenues for potential future diagnostic tools.

## 2. Materials and methods

### 2.1. Gene co-expression analysis

Transcriptome data from human brain tissue was obtained from the Genotype-Tissue Expression Project (GETx) database [23]. Pearson's correlation coefficient (PCC) was employed to explore the presence of a co-expression relationship between two genes.

### 2.2. Human study participants

A two-stage study design was implemented in this study for disease-gene-variant association analysis. A total of 1084 study participants, including 452 SCZ cases and 632 controls, were enrolled in the study. In the first stage, 60 SCZ cases (30 patients with first-episode SCZ and 30 patients with chronic SZ) and 60 controls (age- and sex-matched controls) were recruited to verify the alteration in the mRNA levels of *SART3*, *RNF4*, and *NRF2*. After expression changes were confirmed, a second-stage study with 392 SCZ cases and 572 controls was conducted to investigate the genetic association of targeted SNPs in *SART3* and *RNF4* genes. The participants in the two study stages ($n = 120$ and $n = 964$) did not overlap. All participants were recruited at the Shanghai Mental Health Center between September 2019 and April 2022, and the cohort was approved by the institutional ethics committee (No. 2019–35R). Written informed consent was obtained from all participants following the Declaration of Shanghai Mental Health Center.

All enrolled patients satisfied the following criteria: (a) Han Chinese individuals aged between 18 and 65 years; (b) strict DSM-IV diagnosis by two experienced psychiatrists, with the Mini International Neuropsychiatric Interview (MINI) used as a screening scale; (c) having no substance-induced psychotic disorders, traumas, head injuries, or any other psychotic symptom except SCZ. PANSS was utilized to assess SCZ clinical assessments in patients. Healthy controls were recruited through advertisements in the local hospital at the same time and excluded if they had a personal or family history of mental illness, neurological disorder, head injury leading to loss of consciousness, alcohol or substance abuse, or an intelligence quotient (IQ) $< 70$ (Fig. S1).

### 2.3. Real-time quantitative RT-PCR

Total RNA from 60 peripheral blood samples (60 SCZ patients and 60 healthy controls from the first stage) was isolated with the QIAamp RNA Blood Mini Kit (Qiagen, Chatsworth, CA, USA), and cDNA was synthesized for real-time PCR using the PrimeScript RT reagent kit (Takara). The mRNA levels of SART3 and RNF4 were measured by real-time quantitative RT-PCR with the results normalized to glyceraldehyde phosphate dehydrogenase (GAPDH), using Light Cycler ®480 SYBR Green PCR Master Mix (Roche, USA) with 384-well format according to the standard manufacturer's protocol. All primers used were as follows:*SART3*-F: 5′-CAGCTGGAGAAACACAAAATGT-3'; *SART3*-R: 5′-GTAGCAGTAACCTCGGAAATCC-3'; *RNF4*-F: 5′-GAGCCTGTGGTGGTTGAT-3'; *RNF4*-R: 5′-ATTCCTCCTTGGTCTTCTTCTT-3'; *NRF2*-F: 5′-CACATCCAGTCAGAAACCAGTGG-3'; *NRF2*-R: 5′- GGAATGTCTGCGC-CAAAAGCTG-3'; *GAPDH*-F: 5′-GTCAGCCGCATCTTCTTTTG-3'; *GADPH*-R: 5′-GCGCCCAATACGACCAAATC-3'.

### 2.4. SNP selection and genotyping

We extracted all SNPs with minor allele frequency (MAF) ≥0.05 within the region of the *RNF4* and *SART3* genes according to the data in 1000 Genomes from the Chinese Han population. Pairwise $r^2 \geq 0.8$ was used as the criteria for tag SNP selection. A total of nine tag SNPs, three in *SART3* and six in *RNF4*, met the criteria and were included in the association analyses. Detailed information about these nine selected SNPs is listed in Supplementary Table S1. Genomic DNA was extracted from peripheral blood leukocytes using Tiangen DNA isolation kits (Tiangen Biotech, Beijing, China) and was stored at −80 °C until genotyping.

### 2.5. Statistical analysis

The sample size for this study was calculated using Quanto software (Version 1.2.4) [24] based on the prevalence of SCZ (1 %) and a moderate effect size of odds ratio (1.5). The inheritance model was set as additive, and the sample size of the case-control study was set to be unmatched. The statistical power of the sample is above 95 % as the minor allele frequency (MAF) of the selected SNPs ranged from 24 % to 34 % (at $\alpha = 0.05$), as shown in Table S2. An a priori power analysis was performed to calculate the study sample size using G*Power software (Version 3.1.9.7) [25]. The analysis revealed that a sample of 676 participants across two groups was sufficient to observe the association between SNP and SCZ ($\alpha = 0.05$, a medium effect of 0.25, and a power of 0.90). Our present study's sample size is adequate to test the hypotheses.

The independent sample *t*-test and the $\chi^2$ test were used to compare continuous and categorical variables. Hardy–Weinberg equilibrium testing among the SNPs was evaluated using the online software SNPstats (https://www.snpstats.net/start.htm) [26]. Case-control association analyses were calculated using SHEsis (http://analysis.bio-x.cn) [27] and SNPstats.

Furthermore, the multifactor-dimensionality reduction (MDR) method was applied to estimate the effect of gene-gene interactions on SCZ [28]. This approach incorporates genotypes associated with lower and higher predisposition into two groups of low-risk and high-risk combinations, respectively. The combination with the lower misclassification is considered the better model. Additionally, the predictive ability of all models is assessed using 10-fold cross-validation. Ultimately, the optimal model was identified based on the maximum cross-validation consistency. Hierarchical interaction graphs and interaction dendrogram generated by MDR were employed to illustrate the gene interactions in the best model.

All P-values were two-tailed, and P-values<0.05 were considered statistically significant. Bonferroni corrections were applied to address multiple comparisons. The PLINK tool was used to construct Linkage disequilibrium (LD) blocks based on data from the discovery stage and to perform haplotype-based analyses [29].

### 2.6. HEK293T cell culture

We selected the HEK293T cell line based on its high transfection efficiency. Furthermore, in interaction proteomics, HEK293 cells are widely recognized as a "gold standard" for investigating protein–protein interactions [30–32]. HEK293T cells were cultured in Dulbecco's modified Eagle's medium (Gibco BRL, Carlsbad, CA) supplemented with 10 % fetal bovine serum in a 37 °C humidified incubator with 5 % $CO_2$.

### 2.7. Plasmid construction and transfection

*SART3* and *RNF4* were cloned from human blood cDNA using PCR. The primers were as follows: *SART3*: 5′-CGCGGGCCCGGGATCATGGCGACTGCGGCCGAA-3′ and 5′-TAGATCCGGTGGATCTCACTTTCTCAGAAACAGCT-3' (*Bam*HI sites in bold), *RNF4*: 5′-CGCGGGCCCGGGATCATGAGTACAAGAAAGCGTCG-3′ and 5′-TAGATCCGGTGGATCTCATATATAAATGGGGTGGTA-3' (*Bam*HI sites in bold). Then, the PCR products were cloned in a frame with modified cherry (mCherry) and enhanced green fluorescent protein (EGFP) in an empty plasmid, respectively, for generating mCherry-SART3 and EGFP-RNF4.

According to the manufacturer's instructions, HEK293T Cells were transfected with siRNA against SART3 or the constructed plasmid mCherry-SART3 using Lipofectamine 2000 (Invitrogen, USA).

### 2.8. Immunofluorescence and immunoprecipitation (CoIP)

For analysis by fluorescence microscopy, cells were cultured and transfected onto coverslips. The slices were washed with 1 % 1 × PBS and incubated with 4 % paraformaldehyde solution (Sangon, China) for 10 min. Then, the slices were washed with 1 % 1 × PBS and stained with 4',6-diamidino-2-phenylindole (DAPI, 1: 1000; Sigma, St. Louis, MO, USA) for 15 min at room temperature. After washing in 1 % 1 × PBS three times, the slides were mounted with DPX Mountant and examined by confocal microscope (Leica, TCS SP2, Germany).

Cells were collected and homogenized in lysis buffer (50 mM Tris/HCl, pH 7.5, 150 mM NaCl, one mM EDTA, 0.1 % NP-40, and protease inhibitor cocktail). Pre-cleared samples were immunoprecipitated overnight with a GFP antibody. Immunocomplexes were recovered using protein A or G-agarose and analyzed by immunoblotting using antibodies against SART3 and RNF4 antibodies.

The antibodies used in this study include rabbit SART3(1:2000, Abcam' RabMAb ® technology), GFP (1:2000), and β-actin (1:5000).

## 3. Results

### 3.1. Association of SART3 and RNF4 in SCZ patients

Our previous study identified a set of differentially expressed genes, including *SART3* and *RNF4*, between SCZ and controls [9]. To investigate the relationship between these genes, we performed co-expression analysis using the transcriptome data from human brain tissue, which was obtained from the GETx database and found that *SART3* and *RNF4* exhibited the highest co-expression value (Pearson's correlation coefficient, PCC values = 0.87) among all the genes in the brain (Fig. 1A), indicating a potential genetic interaction between these two genes.

Thus, we recruited 30 patients with first-episode SCZ and 30 patients with chronic SCZ, as well as 60 healthy controls matched for their age and sex. Peripheral blood was obtained from all individuals for analysis of mRNA levels. We observed significantly elevated mRNA levels of *RNF4* and *SART3* in first-episode SCZ patients compared to age- and sex-matched controls (all $P < 0.0001$, Fig. 1B, see methods). We also observed that mRNA levels of both *RNF4* and *SART3* were significantly increased in the peripheral blood of chronic SCZ patients compared to controls (all $P < 0.0001$, Fig. 1C, see methods). These results suggest that *RNF4* and *SART3* exhibit abnormal expression patterns in SCZ patients and would be a logical relationship to investigate further for their involvement in SCZ etiology.

### 3.2. Interaction of SART3 and RNF4 gene polymorphisms on SCZ risk

Common variants, such as SNPs discovered from genome-wide association studies (GWAS), have been proven important risk factors in SCZ [33]. Here, we recruited 392 SCZ patients and 572 controls to investigate whether polymorphisms of *SART3* and *RNF4*

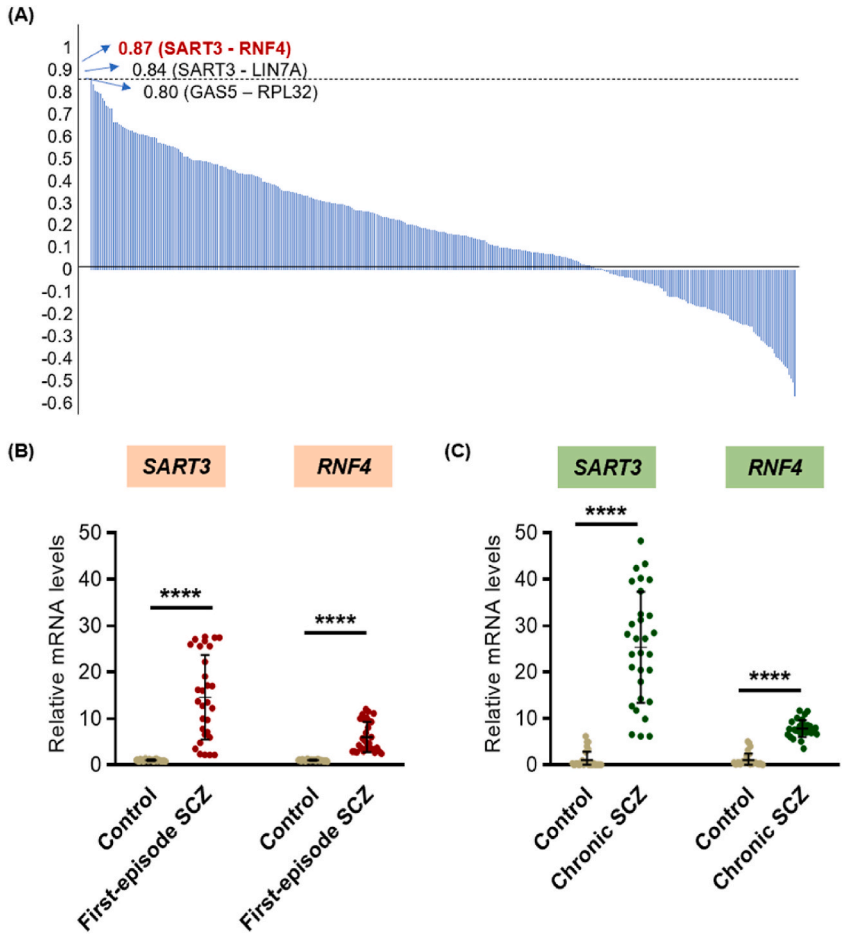


**Fig. 1.** PPC value and the mRNA levels of RNF4 and SART3. A. Comparison of PCC value of gene pairs correlated with SCZ. The plot showed highly co-expressed gene pairs in the brain (PCC≥0.8 based on the brain expressions from GTEx). B. The mRNA level of RNF4 and SART3 in first-episode SCZ cases vs age- and sex-matched controls. n = 30 per group. C. The mRNA level of RNF4 and SART3 in chronic SCZ cases vs. age- and sex-matched controls. n = 30 per group. ****$P < 0.0001$. STAR3: Squamous cell carcinoma antigen recognized by T cells 3. RNF4: Ring finger protein 4. LIN7A: Lin-7 Homolog A. GAS5: Growth arrest-specific 5. RPL32: Ribosomal protein L32. SCZ: Schizophrenia. PCC: Pearson correlation coefficient. GTEx: Genotype-Tissue Expression.

could contribute to the SCZ risk. By performing the $\chi^2$ test and the independent sample *t*-test, we observed no difference in gender (male/female 220/172 vs. 300/272, $P = 0.261$) and age ($33.1 \pm 7.4$ vs. $33.9 \pm 7.8$, $P = 0.097$) distributions between SCZ and control groups (Supplementary Table S3). Next, based on previous studies [34], we selected three tag-SNPs located within intronic regions of *SART3* and six tag-SNPs within intronic regions of *RNF4* for DNA analysis (Fig. 2A). Analysis of pairwise LD ($r^2$>0.8) was then performed for all selected tag SNPs in *SART3* and *RNF4* by using Haploview [35] (Fig. 2B–Supplementary Table S4). The distributions of genotypes in control subjects were consistent with Hardy-Weinberg equilibrium in both *RNF4* ($P > 0.05/6$) and *SART3* ($P > 0.05/3$) genes (Table S5).

The association analysis between the polymorphisms and the risk of SCZ showed that only the C/C–C/A of *RNF* [rs1203860] under the recessive model had a higher risk of SCZ (OR = 2.66 [1.35–5.23], p = 0.0041, Table 1). However, single-SNP-based association analysis under other models showed no significant differences in any of the SNPs from the SART3 and RNF4 genes between SCZ cases and controls (Table 1 and Supplementary Table S6). Similarly, the haplotype-based analysis showed no significant association between haplotypes from the SART3 or RNF4 genes and SCZ (Supplementary Table S7).

When considering combination models of *SART3* and *RNF4*, we identified a significant maximum balanced accuracy of one 3-loci model (*SART3* [rs2287550] - *RNF4* [rs1203860, rs2282765]) at $p < 0.001$ level (OR = 1.74 [1,33-2.26]) with the permutation test of 10,000 iterations (Table 2). The 3-loci model showed the highest accuracy (Accuracy = 58.61 %, Table 2) compared to other models. Next, we performed the 3-loci genotype combination analysis with high-risk and low-risk for SCZ in each multi-loci genotype combination. As a result, a total of 10 high-risk locus combination models and nine low-risk locus combination models were determined by MDR (Fig. 2C). These results provide further evidence of the involvement of *SART3* and *RNF4* interaction in SCZ.

### 3.3. *SART3 downregulates the expression of RNF4 by ubiquitination*

Our model for predicting the occurrence of SCZ showed a combined action of both genes to increase the risk of SCZ, while any single one was insufficient to cause a change. Thus, we next explored whether there is a biological interaction between SART3 and RNF4 in HEK293T cells. Since the protein association is critically determined by subcellular localization, the first step is to clarify their locations by immunofluorescence assay (IFA). We first transfected GFP-RNF4 and mCherry-SART3 plasmids in HEK293T cells. We observed RNF4 strongly localized to both the nucleus and cytoplasm in IFA, whereas SART3 was strongly localized to the nucleus and

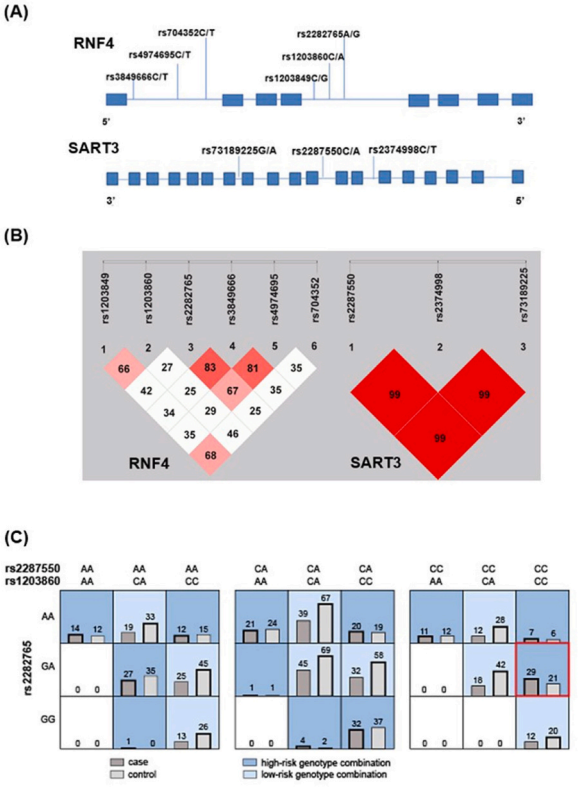


**Fig. 2.** Genetic association between *RNF4* and *SART3* SNPs A. Locations of SNPs in RNF4 and SART3 genes. B. Pairwise linkage disequilibrium results among SNPs in RNF4 and SART3. C. The distribution of high-risk, low-risk genotype combinations and hierarchical interaction graphs as well as interaction dendrogram in the best three locus model of RNF4(rs1203860, rs2282765) and SART3(rs2287550), OR = 1.94[1.08–3.49]. STAR3: Squamous cell carcinoma antigen recognized by T cells 3. RNF4: Ring finger protein 4. OR: odds ratio.

**Table 1a**
Genotype distributions of *RNF4* functional polymorphisms in SCZ and all HC.

| SNPs | Models | Genotype | OR (95 % CI) | P value |
|---|---|---|---|---|
| rs3849666 | Dominant | C/C vs C/T-T/T | 0.96 (0.65–1.43) | 0.84 |
| | Recessive | C/C–C/T vs T/T | 0.77 (0.43–1.38) | 0.37 |
| | Additive | – | 0.92(0.69–1.22) | 0.56 |
| rs4974695 | Dominant | T/T vs C/T-C/C | 1.02 (0.68–1.54) | 0.92 |
| | Recessive | T/C–C/T vs C/C | 0.96 (0.56–1.65) | 0.89 |
| | Additive | – | 1.00 (0.76–1.32) | 1.00 |
| rs704352 | Dominant | C/C vs C/T-T/T | 1.46 (0.95–2.24) | 0.08 |
| | Recessive | C/C–C/T vs T/T | 1.50 (0.88–2.56) | 0.14 |
| | Additive | – | 1.34(1.00–1.79) | 0.047 |
| rs1203849 | Dominant | C/C vs G/C-G/G | 1.18 (0.77–1.82) | 0.44 |
| | Recessive | C/C-G/C vs G/G | 1.54 (0.91–2.60) | 0.11 |
| | Additive | – | 1.23 (0.92–1.63) | 0.16 |
| rs1203860 | Dominant | C/C vs C/A-A/A | 0.90 (0.60–1.35) | 0.61 |
| | Recessive | C/C–C/A vs A/A | 2.66 (1.35–5.23) | **0.0041** |
| | Additive | – | 1.16 (0.85–1.57) | 0.35 |
| rs2282765 | Dominant | A/A vs G/A-G/G | 0.96 (0.64–1.43) | 0.84 |
| | Recessive | A/A-G/A vs G/G | 0.85 (0.49–1.48) | 0.58 |
| | Additive | – | 1.94 (0.71–1.24) | 0.67 |

Notes: RNF4: Ring finger protein 4. SCZ: Schizophrenia. HC: Healthy control. SNP: Single nucleotide polymorphism. OR: odds ratio. CI: Confidence interval.

**Table 1b**
Genotype distributions of *SART3* functional polymorphisms in SCZ and all HC.

| SNPs | Models | Genotype | OR (95 % CI) | P value |
|---|---|---|---|---|
| rs73189225 | Dominant | A/A vs G/A-G/G | 1.03 (0.66–1.61) | 0.91 |
| | Recessive | A/A-G/A vs G/G | 0.76 (0.47–1.23) | 0.27 |
| | Additive | – | 0.92 (0.69–1.22) | 0.56 |
| rs2287550 | Dominant Recessive | A/A vs C/A-C/C | 1.00 (0.64–1.56) | 1.00 |
| | | A/A-C/A vs C/C | 0.74 (0.45–1.20) | 0.22 |
| | Additive | – | 0.90 (0.67–1.0) | 0.46 |
| rs2374998 | Dominant Recessive | T/T vs T/C–C/C | 1.00 (0.64–1.56) | 1.00 |
| | | T/T-T/C vs C/C | 0.72 (0.45–1.16) | 0.18 |
| | Additive | – | 0.89 (0.67–1.18) | 0.42 |

Notes: STAR3: Squamous cell carcinoma antigen recognized by T cells 3. SCZ: Schizophrenia. HC: Healthy control. SNP: Single nucleotide polymorphism. OR: odds ratio. CI: Confidence interval.

**Table 2**
The best model for predicting the occurrence of the SCZ.

| Best model | Balanced accuracy (%) | Accuracy (%) | Sensitivity (%) | CVC | $x^2$ | p-value | OR 95 % CI |
|---|---|---|---|---|---|---|---|
| RNF4 (rs1203860) | 53.08 | 52.18 | 57.91 | 10/10 | 3.56 | 0.003 | 1.28 (0.99–1.66) |
| RNF4 (rs1203860), SART3(rs2287550) | 54.27 | 53.73 | 57.14 | 5/10 | 7.09 | 0.0078 | 1.41 (1.09–1.83) |
| RNF4(rs1203860,rs2282765), SART3 (rs2287550) | 56.49 | 58.61 | 45.15 | 9/10 | 16.74 | <0.0001 | 1.74 (1.33–2.26) |

Notes: STAR3: Squamous cell carcinoma antigen recognized by T cells 3. RNF4: Ring finger protein 4. CVC: Cross validation consistency. OR: odds ratio. CI: Confidence interval.

weakly to the cytoplasm. By merging results, we observed that both proteins emphasize the co-localization of the nucleus of the cell (Fig. 3A). Next, to further investigate the protein-protein interactions between RNF4 and SART3, we performed a CoIP assay using lysates from HEK293T cells transfected with plasmids expressing GFP or GFP-RNF4. The lysates were incubated with anti-GFP antibodies, and the immunoprecipitates were probed with anti-SART3 antibodies by Western blot analysis. Our results showed that SART3 co-immunoprecipitated with RNF4, indicating a direct interaction between the two proteins (Fig. 3B).

To explore the regulatory relationship between SART3 and RNF4, we transfected HEK293T cells with SART3 siRNA (Si-SART3#1 or Si-SART3#2) or non-targeting control siRNA. After 48 h, we measured the expression levels of RNF4 protein by Western blot analysis. Our results showed that the knockdown of SART3 using siRNA resulted in a significant increase in the expression of RNF4 at the protein levels by approximately 1.63-fold compared to control cells (Fig. 3C). Then, we transfected HEK293T cells with mCherry-SART3 or an empty vector control. The overexpression of STAT3 led to a significant decrease in RNF4 protein level by approximately

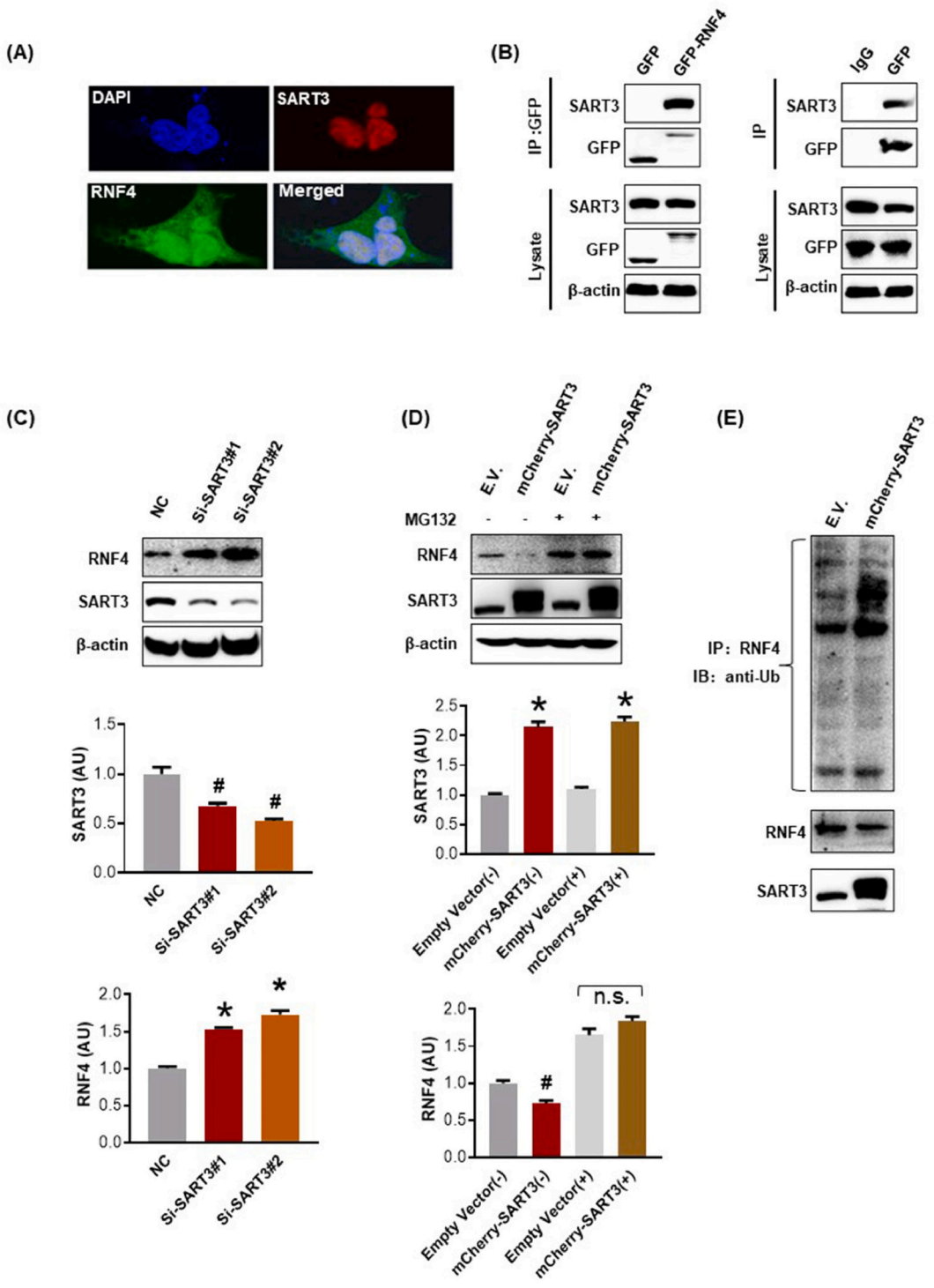


*(caption on next page)*

**Fig. 3.** SART3 negatively regulates RNF4 by ubiquitination A. Co-localization of SART3 and RNF4. 293T cells were transfected with mCherry-SART3 and eGFP-RNF4. Images were taken with a confocal microscope (Olympus) (scale bar:10 μm). B. The left side of the panel shows the IB analysis of lysate and IPs derived from 293T cells transfected with the GFP or GFP-RNF4 constructs. The right side of panel B shows the IB analysis of lysate and IPs derived from 293T cells transfected with GFP-RNF4 constructs. IgG was used as a negative control. C. IB analysis of lysate derived from 293T cells transfected siRNA against SART3. D. IB analysis of lysate derived from 293T cells transfected with the indicated constructs E.V. or mCherry-SART3. Where indicated, MG132 (20 μM) was treated for 8h. E. IB analysis of RNF4 ubiquitin and lysate derived from 293T cells transfected with the indicated constructs. *P < 0.05 shows an increase versus vehicle or control; #P < 0.05 shows a reduction versus vehicle or control; n.s. means no significance. STAR3: Squamous cell carcinoma antigen recognized by T cells 3. RNF4: Ring finger protein 4. DAPI: 4′,6-Diamidino-2′-phenylindole. IP: Immunoprecipitation. IB: Immunoblotting. IgG: Immunoglobulin G. GFP: Green fluorescent protein. NC: Negative control. Si-SART3: The small interference RNA targeting SART3. E.V.: Empty vector. mCherry-SART3: mCherry and SART3 expression plasmid. AU: Area units. Anti-Ub: Anti-Ubiquitin antibody.

1.38-fold compared to control cells (Fig. 3D). Previous studies have shown that SART3 is involved in ubiquitination [36]. Therefore, we considered that the SART3-mediated downregulation of RNF4 might be through the ubiquitination pathway. Therefore, we treated HEK293T cells with MG132, a proteasome inhibitor, to investigate whether SART3 mediates RNF4 downregulation via the ubiquitination pathway. We found that the RNF4 protein level showed no change after the overexpression of STAT3 compared to control cells in the condition of MG132 (Fig. 3D). Moreover, we detected the ubiquitination of endogenous RNF4 after the overexpression of STAT3. Our results showed that overexpression of STAT3 led to a considerable increase in endogenous RNF4 ubiquitination compared to control cells (Fig. 3E), suggesting that STAT3-mediated RNF4 protein degradation occurs through the induction of RNF4 ubiquitination.

### *3.4. SART3 downregulates the expression of NRF2, a downstream factor of RNF4*

To gain further insights into the regulatory network and signaling pathways associated with the biological process under

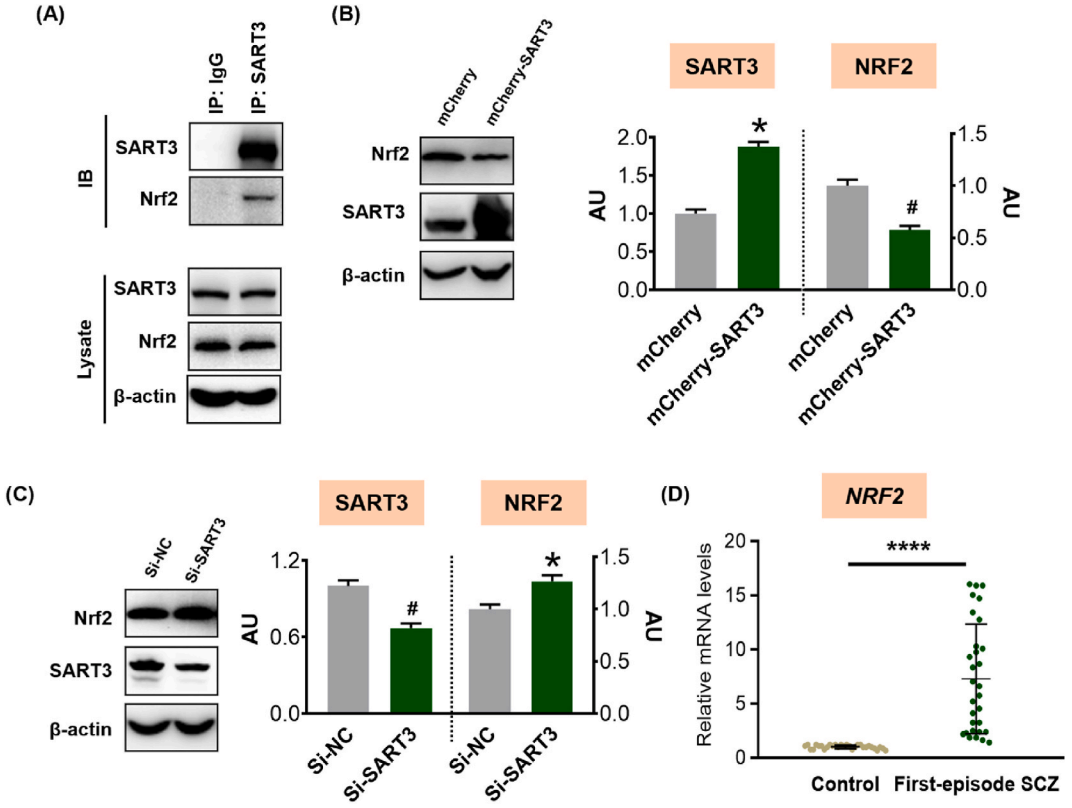


**Fig. 4.** SART3 regulates the expression of NRF2 (A) IB analysis of lysate and IPs derived from 293T cells. IgG was used as a negative control. (B) IB analysis of lysate derived from 293T cells with transfected the indicated constructs. E.V. or mCherry-SART3. (C) IB analysis of lysate derived from 293T cells with transfected siRNA against SART3. (D) The mRNA expression level of NRF2 in first-episode SCZ cases vs age- and sex-matched controls (n = 30). *P < 0.05 shows an increase versus vehicle or control; #P < 0.05 shows a reduction versus vehicle or control; ****P < 0.0001. STAR3: Squamous cell carcinoma antigen recognized by T cells 3. Nrf2: Nuclear factor E2-related factor 2. IP: Immunoprecipitation. IB: Immunoblotting. IgG: Immunoglobulin G. Si-NC: The small interference RNA negative control. Si-SART3: The small interference RNA targeting SART3. mCherry-SART3: mCherry and SART3 expression plasmid. AU: Area units. SCZ: Schizophrenia.

investigation, we investigated the effect of SART3 on NRF2, a downstream factor of RNF4 involved in the process. Previous studies have demonstrated NRF2 degradation's dependency on the sumo-specific E3 ubiquitin ligase RNF4 [14]. However, SART3 may regulate NRF2 independently from RNF4. To explore this, we first detected the interaction between SART3 and NRF2. We used lysates from HEK293T cells to perform a CoIP assay and determined immunoprecipitates by probing with anti-NRF2 antibodies via Western blot analysis after treating with anti-SART3 antibodies. The results demonstrated that SART3 can co-precipitate with NRF2 (Fig. 4A), indicating a direct interaction between the two proteins.

Subsequently, we transfected HEK293T cells with either empty vector control or mCherry-SART3 to investigate the regulatory relationship between SART3 and NRF2. Compared to control cells, there was a significant decrease of approximately 1.74-fold in NRF2 protein levels after overexpression of STAT3 (Fig. 4B). Simultaneously, we transfected HEK293T cells with either non-targeting control siRNA or SART3 siRNA. After 48 h, we quantified NRF2 protein expression levels using Western blot analysis. The results demonstrated that knocking down SART3 using siRNA led to a substantial increase of approximately 1.27-fold in the protein level expression of RNF4 compared to control cells (Fig. 4C), suggesting that SART3 directly inhibited the expression of NRF2.

To further investigate whether abnormal expression of NRF2 existed in patients with SCZ, we used the blood samples from 30 first-episode patients with SCZ and 30 age- and sex-matched controls, which were recruited from the first study stage. The mRNA levels of *NRF2* were detected. Our results showed that the expression of mRNA level of *NRF2* in first-episode SCZ patients was significantly higher than controls (Fig. 4D), suggesting that similar to *RNF4* and *SART3*, *NRF2* was also aberrantly expressed in SCZ patients.

## 4. Discussion

Historically, the focal point of research in the realm of SCZ has predominantly revolved around the discussion of protein-coding genes [37]. Our study observed a co-expression relationship between the *RNF4* and *SART3* genes in the human brain transcriptome, characterized by a notably high PCC. In a pioneering endeavor, we have identified a 3-loci SNP model encompassing *RNF4* and *SART3*, which heightens susceptibility to SCZ. Moreover, we have subsequently ascertained that SART3 exerts regulatory control over the RNF4 signaling pathway through the mechanism of ubiquitination, also exerting a direct influence on NRF2.

In our investigation, we utilized brain tissue transcriptional expression profiling data to investigate the correlation between differentially expressed genes in SCZ patients. Notably, among all the genes examined, *SART3* and *RNF4* possessed the highest co-expression value. This finding underscores a substantial and noteworthy correlation, indicating a robust co-expression between the RNF4 and SART3 genes at the transcriptional level. Elevated mRNA levels of *RNF4* and *SART3* in SCZ patients compared to normal individuals further corroborated this result. Previous studies have supported the pivotal role played by gene co-expression networks in the development of intricate brain diseases, including SCZ [38]. The outcomes of our transcriptional-level data analysis thus provide invaluable insights into the subsequent pathogenic mechanisms underpinning genes that confer susceptibility to SCZ.

Previously reported findings have highlighted the association of the SNP locus rs1203847 of *RNF4* with SCZ [39]. Furthermore, microarray analysis conducted on prefrontal SCZ tissue indicated an elevation in *SART3* expression [40,41]. Additionally, RNA sequencing analysis on ventrolateral prefrontal regions in SCZ patients has implicated the *SART3* enrichment pathway in the pathological process [42]. Our extensive investigation meticulously assessed a substantial clinical sample comprising SCZ patients and control subjects to detect SNPs within *RNF4* and *SART3*. We found that the rs1203860 of *RNF4* under the recessive model was independently associated with SCZ susceptibility. Despite the absence of a significant correlation between these two genes and SCZ through single-SNP genetic association analysis under other models and haplotype-based analysis, our gene-gene interaction analysis unveiled that rs1203860 (*RNF4*), rs2282765 (*RNF4*), and rs2287550 (*SART3*) possess the potential to serve as robust predictors of SCZ. Consequently, it becomes evident that the interaction between *RNF4* and *SART3* accentuates susceptibility to SCZ. It is essential to recognize that SCZ does not adhere to a Mendelian pattern of inheritance but rather manifests as a complex disease precipitated by a multitude of subtle effects and the involvement of multiple genes [43]. In light of these complexities, it is imperative for future research to prioritize the exploration of networks as opposed to focusing solely on individual SNPs.

Since Mah et al. conducted the first GWAS on SCZ in 2006 [44], European SCZ GWAS has consistently led the global forefront. For instance, the Psychiatric Genomics Consortium (PGC) conducted multiple GWAS analyses in 2011 [45], 2013 [46], 2014 [3], and 2022 [2], revealing numerous risk genes associated with SCZ. Our comparison with previous large-scale GWAS did not show an overlap between our selected genes (*RNF4* and *SART3*) and known databases. However, within the RNF family, where *RNF4* is included, several genes (*RNF168*, *RNF208*, *RNF34,* and *RNF7*) have been identified as susceptible genes [2], indicating a potential association. In the future, it is essential to conduct an in-depth exploration of GWAS based on the Chinese or Asian populations.

Our IFA results have elucidated the subcellular distribution patterns of RNF4 and SART3. Specifically, RNF4 was widely distributed in both the nucleus and cytoplasm, while SART3 predominantly resided within the nucleus. These findings align with previous reports [12,47]. Importantly, it is well-established that dysregulation or malfunction of RNF4 and SART3 can disrupt the regulation of nuclear signaling, thereby giving rise to various related diseases [48,49].

Notably, despite the absence of prior reports detailing interactions between these two proteins in databases such as BioGRID [50] and STRING [51] databases, our subsequent Co-IP experiments have unveiled, for the first time, a direct binding interaction between RNF4 and SART3 proteins. Moreover, we discovered that interfering with or overexpressing SART3 resulted in discernible alterations in the expression level of the RNF4 protein. Furthermore, an increase in the ubiquitination level of the RNF4 protein was observed following the overexpression of SART3. Collectively, our study outcomes provide compelling evidence to support the conclusion that SART3 exerts a direct down-regulatory effect on the RNF4 protein through the mechanism of ubiquitination. The protein expressions of RNF4 and SART3 in cells did not align with the RNA expression results in SCZ patients. However, discrepancies between transcriptional and translational levels are a common phenomenon. Moreover, the complex physiological environment of the human body can

also contribute to such disparities.

Subsequently, our investigation delved into the regulatory influence exerted by the SART3 protein on NRF2, a downstream molecule associated with the RNF4 protein. Previous reports have established that RNF4 plays a pivotal role in mediating the degradation of NRF2 [52]. NRF2 activation is instrumental in triggering the expression of genes that fortify cellular defenses in response to stress conditions [53]. It also controls the expression of essential components of the antioxidant system, such as glutathione and thioredoxin, which are integral to maintaining cellular redox homeostasis [54]. RNF4 regulates the homeostatic system of NRF2 via SUMOylation [14]. It is well-recognized that the brain's limited capacity to counteract oxidative stress during critical developmental phases effectively contributes to the emergence of neurodevelopmental abnormalities [55]. Our Co-IP assays substantiate that SART3 and NRF2 proteins interact directly. Furthermore, we observed that SART3 exhibited an inhibitory effect on NRF2. These observations suggest that SART3 exerts an influence on NRF2 independently of RNF4. Nevertheless, it is imperative to conduct further research to elucidate the intricate mechanisms underpinning this process. In summation, our data collectively unveil a complex regulatory interplay between SART3, RNF4, and NRF2, culminating in an elevated risk of SCZ by impacting the oxidative stress response during neurodevelopment. Following clinical validation, the mRNA levels of *NRF2* were increased in the first-episode SCZ patients. The variation in the blood is inconsistent with the findings from cell studies and may be due to the body's compensatory response or other unknown mechanisms. However, the aberrant levels serve as compelling evidence of their role in the disease's onset.

SCZ is a complex multifactorial disorder showing polygenic inheritance. GWAS has identified approximately 500 susceptibility genes related to SCZ [56]; however, the effect of individual genes is small. Gene-gene interaction may be more important in explaining the occurrence of SCZ. Meanwhile, SCZ is related to gene-environment interactions, and the regulation of gene expression level by environmental factors may be more significant than the mutation of gene loci. Therefore, this study focused more on the interaction of gene expression levels. In this study, we found that the interaction between *RNF4* and *SART3* increased the risk of SCZ, especially at the mRNA and protein levels. More importantly, our blood samples from clinical SCZ patients also showed increased expression of RNF4 and SART3. This suggests that the interaction of mRNA and protein expression levels of RNF4 and SART3 has greater potential to be a reliable biomarker.

While our findings provide pioneering evidence supporting the association between RNF4 and SART3 and the risk of SCZ, it's essential to acknowledge the limitations inherent in our study design. In our study, although the association analysis results had significant differences, the accuracies were not high. The balance accuracy of all three SNP models was slightly higher than that of the two-SNP model or the single SNP model. These may be related to the small sample size. The results still need to be further verified by large sample-size studies. Moreover, we did not investigate the mutual regulatory relationship between *RNF4* and *SART3* within neuronal cells or animal models. This limitation curtails our comprehensive understanding of the roles these pathways play in neurodevelopment. Future studies should endeavor to explore the molecular mechanisms and pathways through which *RNF4* and *SART3* contribute to the pathogenesis of SCZ.

In conclusion, our genetic association analysis and molecular experiments both identified the interaction between RNF4 and SART3 as significantly associated with an elevated risk of SCZ. Clinical patient blood data also showed significant increases in the levels of RNF4 and SART3. This discovery highlights the potential of this interaction as a novel molecular biomarker for predicting SCZ risk within our population. This has specific clinical value for the accurate diagnosis and treatment of SCZ. In the follow-up study, we will further validate it in a larger clinical sample and develop a biomarker kit for clinical application. This will assist clinicians to identify early, diagnose accurately, predict disease progression, tailor treatment plans, and provide personalized care to SCZ patients.

## Ethics approval and consent to participate

The cohort was approved by the institutional ethics committee (No. 2019–35R) in September 2019. Written informed consent was obtained from all participants following the Declaration of Shanghai Mental Health Center.

## Data availability statement

Due to ethical approval limitations, the datasets for this article are not publicly available; the summary data is available upon request.

## CRediT authorship contribution statement

**Ying Cheng:** Writing – review & editing, Visualization, Validation, Software, Formal analysis. **Xi Chen:** Writing – review & editing, Writing – original draft, Visualization, Conceptualization. **Xiao Qing Zhang:** Methodology, Investigation, Formal analysis, Data curation. **Pei Jun Ju:** Writing – original draft, Methodology, Investigation, Data curation. **Wei Di Wang:** Writing – original draft, Software, Methodology, Data curation. **Yu Fang:** Writing – original draft, Methodology, Formal analysis. **Guan Ning Lin:** Writing – review & editing, Writing – original draft, Methodology, Funding acquisition, Formal analysis, Data curation, Conceptualization. **Dong Hong Cui:** Writing – review & editing, Supervision, Resources, Project administration, Methodology, Investigation, Funding acquisition, Data curation, Conceptualization.

## Declaration of generative AI and AI-assisted technologies in the writing process

During the preparation of this work, the authors used ChatGPT to improve language and readability. After using this tool, the

authors reviewed and edited the content as needed and took full responsibility for the content of the publication.

## Declaration of competing interest

The authors declare that they have no known competing financial interests or personal relationships that could have appeared to influence the work reported in this paper.

## Acknowledgments

Our gratitude is expressed to the patients and their families for participation in the clinical study. We also thank Dr. Xiao Fang Cui for her valuable assistance and help during the preparation of this article. The study was supported by grants from the National Key R&D Program of China (No: 2017YFC0909200); the National Natural Science Foundation of China (No: 82271544) for Dong Hong Cui, and also the 2030 Science and Technology Innovation Key Program of the Ministry of Science and Technology of China (No. 2022ZD020910001); the National Natural Science Foundation of China (No: 81971292, 82150610506); Natural Science Foundation of Shanghai (No: 21ZR1428600); the Medical-Engineering Cross Foundation of Shanghai Jiao Tong University (No: YG2022ZD026 and YG2023ZD27) for Guan Ning Lin. We also appreciate the support from the China Scholarship Council (No: 202106230212) to Xi Chen.

## Appendix A. Supplementary data

Supplementary data to this article can be found online at https://doi.org/10.1016/j.heliyon.2024.e32743.

## References

[1] A.S. Brown, The environment and susceptibility to schizophrenia, Prog. Neurobiol. 93 (1) (2011) 23–58.
[2] V. Trubetskoy, et al., Mapping genomic loci implicates genes and synaptic biology in schizophrenia, Nature 604 (7906) (2022) 502–508.
[3] Biological insights from 108 schizophrenia-associated genetic loci, Nature 511 (7510) (2014) 421–427.
[4] M.H. Nia, et al., Relationship between P2XR4 gene variants and the risk of schizophrenia in south-East of Iran: a preliminary case-control study and in silico analysis, Iran. J. Public Health 50 (5) (2021) 978–989.
[5] M. Heidari Nia, et al., Relationship between GABRB2 gene polymorphisms and schizophrenia susceptibility: a case-control study and in silico analyses, Int. J. Neurosci. 132 (6) (2022) 633–642.
[6] S. Sargazi, et al., Association of a novel KIF26B gene polymorphism with susceptibility to schizophrenia and breast cancer: a case-control study, Iran. J. Public Health 50 (2) (2021) 397–406.
[7] S. Sargazi, et al., Impact of proliferator-activated receptor γ gene polymorphisms on risk of schizophrenia: a case-control study and computational analyses, Iran. J. Psychiatry 15 (4) (2020) 286–296.
[8] S. Sargazi, et al., Relationship between single nucleotide polymorphisms of GRHL3 and schizophrenia susceptibility: a preliminary case-control study and bioinformatics analysis, Int J Mol Cell Med 9 (2) (2020) 154–164.
[9] D.H. CuiH.Y, X.Y. Wang, B. Zhu, K.D. Jiang, Microarray analysis of altered gene expression in schizophrenia, Chinese Journal of Psychiatry 37 (1) (2004) 4–8.
[10] M. Fromer, et al., De novo mutations in schizophrenia implicate synaptic networks, Nature 506 (7487) (2014) 179–184.
[11] L. Chiariotti, et al., Identification and characterization of a novel RING-finger gene (RNF4) mapping at 4p16.3, Genomics 47 (2) (1998) 258–265.
[12] N. Galili, et al., Rnf4, a RING protein expressed in the developing nervous and reproductive systems, interacts with Gscl, a gene within the DiGeorge critical region, Dev. Dynam. 218 (1) (2000) 102–111.
[13] L. Guo, A Cellular System that Degrades Misfolded Proteins through Sequential Sumoylation and Ubiquitination, 2013.
[14] N. Komaravelli, et al., Respiratory syncytial virus induces NRF2 degradation through a promyelocytic leukemia protein - ring finger protein 4 dependent pathway, Free Radic. Biol. Med. 113 (2017) 494–504.
[15] T. Nagase, et al., Prediction of the coding sequences of unidentified human genes. IV. The coding sequences of 40 new genes (KIAA0121-KIAA0160) deduced by analysis of cDNA clones from human cell line KG-1, DNA Res. 2 (4) (1995) 167–174.
[16] Y. Liu, et al., C-MYC controlled TIP110 protein expression regulates OCT4 mRNA splicing in human embryonic stem cells, Stem Cell. Dev. 22 (5) (2013) 689–694.
[17] Y. Liu, et al., Tip110 maintains expression of pluripotent factors in and pluripotency of human embryonic stem cells, Stem Cell. Dev. 21 (6) (2012) 829–833.
[18] J.P. Petschek, et al., RNA editing in Drosophila 4f-rnp gene nuclear transcripts by multiple A-to-G conversions, J. Mol. Biol. 259 (5) (1996) 885–890.
[19] X.V. Hu, et al., Identification of RING finger protein 4 (RNF4) as a modulator of DNA demethylation through a functional genomics screen, Proc. Natl. Acad. Sci. U. S. A. 107 (34) (2010) 15087–15092.
[20] N.S. Trede, et al., Network of coregulated spliceosome components revealed by zebrafish mutant in recycling factor p110, Proc. Natl. Acad. Sci. U. S. A. 104 (16) (2007) 6608–6613.
[21] A. Whitmill, et al., Tip110 deletion impaired embryonic and stem cell development involving downregulation of stem cell factors nanog, Oct4, and Sox2, Stem Cell. 35 (7) (2017) 1674–1686.
[22] I. Iossifov, et al., The contribution of de novo coding mutations to autism spectrum disorder, Nature 515 (7526) (2014) 216–221.
[23] L.J. Carithers, H.M. Moore, The genotype-tissue expression (GTEx) Project, Biopreserv. Biobanking 13 (5) (2015) 307–308.
[24] W. Gaudeman, J. Morrison, Quanto 1.2. 4: a Computer Program for Power and Sample Size Calculations for Genetic-Epidemiology Studies, University of Southern California, 2019.
[25] H. Kang, Sample size determination and power analysis using the G* Power software, Journal of educational evaluation for health professions (2021) 18.
[26] X. Solé, et al., SNPStats: a web tool for the analysis of association studies, Bioinformatics 22 (15) (2006) 1928–1929.
[27] Y.Y. Shi, L. He, SHEsis, a powerful software platform for analyses of linkage disequilibrium, haplotype construction, and genetic association at polymorphism loci, Cell Res. 15 (2) (2005) 97–98.
[28] M.D. Ritchie, et al., Multifactor-dimensionality reduction reveals high-order interactions among estrogen-metabolism genes in sporadic breast cancer, Am. J. Hum. Genet. 69 (1) (2001) 138–147.
[29] S. Purcell, et al., PLINK: a tool set for whole-genome association and population-based linkage analyses, Am. J. Hum. Genet. 81 (3) (2007) 559–575.
[30] E.L. Huttlin, et al., Dual proteome-scale networks reveal cell-specific remodeling of the human interactome, Cell 184 (11) (2021) 3022–3040.e28.
[31] E.L. Huttlin, et al., The BioPlex network: a systematic exploration of the human interactome, Cell 162 (2) (2015) 425–440.

[32] M. Taipale, et al., A quantitative chaperone interaction network reveals the architecture of cellular protein homeostasis pathways, Cell 158 (2) (2014) 434–448.
[33] H. Stefansson, et al., Common variants conferring risk of schizophrenia, Nature 460 (7256) (2009) 744–747.
[34] S.T. Sherry, et al., dbSNP: the NCBI database of genetic variation, Nucleic Acids Res. 29 (1) (2001) 308–311.
[35] J.C. Barrett, et al., Haploview: analysis and visualization of LD and haplotype maps, Bioinformatics 21 (2) (2005) 263–265.
[36] M. Huang, et al., RNA-splicing factor SART3 regulates translesion DNA synthesis, Nucleic Acids Res. 46 (9) (2018) 4560–4574.
[37] R. Birnbaum, D.R. Weinberger, Genetic insights into the neurodevelopmental origins of schizophrenia, Nat. Rev. Neurosci. 18 (12) (2017) 727–740.
[38] E. Radulescu, et al., Identification and prioritization of gene sets associated with schizophrenia risk by co-expression network analysis in human brain, Mol. Psychiatr. 25 (4) (2020) 791–804.
[39] D. Curtis, et al., Case-case genome-wide association analysis shows markers differentially associated with schizophrenia and bipolar disorder and implicates calcium channel genes, Psychiatr. Genet. 21 (1) (2011) 1–4.
[40] K. Iwamoto, M. Bundo, T. Kato, Altered expression of mitochondria-related genes in postmortem brains of patients with bipolar disorder or schizophrenia, as revealed by large-scale DNA microarray analysis, Hum. Mol. Genet. 14 (2) (2005) 241–253.
[41] S. Narayan, et al., Molecular profiles of schizophrenia in the CNS at different stages of illness, Brain Res. 1239 (2008) 235–248.
[42] M. Mladinov, et al., Gene expression profiling of the dorsolateral and medial orbitofrontal cortex in schizophrenia, Transl. Neurosci. 7 (1) (2016) 139–150.
[43] Y. Wu, Y.G. Yao, X.J. Luo, SZDB: a database for schizophrenia genetic research, Schizophr. Bull. 43 (2) (2017) 459–471.
[44] S. Mah, et al., Identification of the semaphorin receptor PLXNA2 as a candidate for susceptibility to schizophrenia, Mol. Psychiatr. 11 (5) (2006) 471–478.
[45] Genome-wide association study identifies five new schizophrenia loci, Nat. Genet. 43 (10) (2011) 969–976.
[46] S. Ripke, et al., Genome-wide association analysis identifies 13 new risk loci for schizophrenia, Nat. Genet. 45 (10) (2013) 1150–1159.
[47] J. Gu, et al., Isolation and characterization of a new 110 kDa human nuclear RNA-binding protein (p110nrb), Biochim. Biophys. Acta 1399 (1) (1998) 1–9.
[48] I. Novotný, et al., SART3-Dependent accumulation of incomplete spliceosomal snRNPs in cajal bodies, Cell Rep. 10 (3) (2015) 429–440.
[49] M. Diefenbacher, A. Orian, Stabilization of nuclear oncoproteins by RNF4 and the ubiquitin system in cancer, Mol Cell Oncol 4 (1) (2017) e1260671.
[50] R. Oughtred, et al., The BioGRID interaction database: 2019 update, Nucleic Acids Res. 47 (D1) (2019) D529–d541.
[51] D. Szklarczyk, et al., The STRING database in 2021: customizable protein-protein networks, and functional characterization of user-uploaded gene/measurement sets, Nucleic Acids Res. 49 (D1) (2021) D605–d612.
[52] M.T. Malloy, et al., Trafficking of the transcription factor Nrf2 to promyelocytic leukemia-nuclear bodies: implications for degradation of NRF2 in the nucleus, J. Biol. Chem. 288 (20) (2013) 14569–14583.
[53] C. Tonelli, I.I.C. Chio, D.A. Tuveson, Transcriptional regulation by Nrf2, Antioxidants Redox Signal. 29 (17) (2018) 1727–1745.
[54] A.Y. Shih, P. Li, T.H. Murphy, A small-molecule-inducible Nrf2-mediated antioxidant response provides effective prophylaxis against cerebral ischemia in vivo, J. Neurosci. 25 (44) (2005) 10321–10335.
[55] M.E. Rains, et al., Oxidative stress and neurodevelopmental outcomes in rat offspring with intrauterine growth restriction induced by reduced uterine perfusion, Brain Sci. 11 (1) (2021).
[56] W. Yue, X. Yu, D. Zhang, Progress in genome-wide association studies of schizophrenia in Han Chinese populations, NPJ Schizophr 3 (1) (2017) 24.